

SCIENTIFIC REPORTS



OPEN

Dynamic Changes of Functional Pain Connectome in Women with Primary Dysmenorrhea

Received: 04 December 2015

Accepted: 31 March 2016

Published: 19 April 2016

Ting-Hsuan Wu^{1,2,*}, Cheng-Hao Tu^{1,2,*}, Hsiang-Tai Chao^{3,4}, Wei-Chi Li¹, Intan Low⁵, Chih-Ying Chuang², Tzu-Chen Yeh^{1,2}, Chou-Ming Cheng², Chih-Che Chou², Li-Fen Chen^{1,2,5} & Jen-Chuen Hsieh^{1,2}

Primary dysmenorrhea (PDM) is the most prevalent gynecological problem. Many key brain systems are engaged in pain processing. In light of dynamic communication within and between systems (or networks) in shaping pain experience and behavior, the intra-regional functional connectivity (FC) in the hub regions of the systems may be altered and the functional interactions in terms of inter-regional FCs among the networks may be reorganized to cope with the repeated stress of menstrual pain in PDM. Forty-six otherwise healthy PDM subjects and 49 age-matched, healthy female control subjects were enrolled. Intra- and inter-regional FC were assessed using regional homogeneity (ReHo) and ReHo-seeded FC analyses, respectively. PDM women exhibited a *trait-related* ReHo reduction in the ventromedial prefrontal cortex, part of the default mode network (DMN), during the periovulatory phase. The *trait-related* hypoconnectivity of DMN-salience network and hyperconnectivity of DMN-executive control network across the menstrual cycle featured a dynamic transition from affective processing of pain salience to cognitive modulation. The altered DMN-sensorimotor network may be an ongoing representation of cumulative menstrual pain. The findings indicate that women with long-term PDM may develop adaptive neuroplasticity and functional reorganization with a network shift from affective processing of salience to the cognitive modulation of pain.

Primary dysmenorrhea (PDM), or menstrual pain without organic causes, is the most prevalent menstrual complaint of young females. Between 40 to 90% of female adolescents have experienced PDM and 10–20% describe their suffering as so severe and distressing that it requires absence from school or work¹. Notably, otherwise healthy women with PDM often display a higher prevalence of incidental brain findings², particularly of normal variants, when compared with control subjects. Additionally, genetic factors, such as the *brain-derived neurotrophic factor (BDNF)* Val66Met polymorphism, may account for the susceptibility of an individual to PDM³.

We have previously reported that long-term PDM is associated with alterations in brain metabolism and functional connectivity (FC) in pain modulatory systems, as well as in *state-* and *trait-related* structures^{4–7}. *State-related* changes are menstrual pain-primed, whereas *trait-related* changes exist even without symptoms. Notably, pain-related regions, such as the medial prefrontal cortex (mPFC), posterior cingulate cortex and insula, exhibit abnormal functional and structural changes in otherwise healthy women with PDM^{4,6,8}. These regions are parts of the pain matrix⁹ and are associated with cognitive control of emotions, self-referential processing¹⁰, contextualizing^{11,12} and pain generation and modulation^{13,14}.

Many key brain systems are engaged for menstrual pain processing; many key regions of these systems are also neural substrates of pain matrix that participate substantially in central processing of pain. Recent studies have demonstrated that the FC of large-scale brain systems/networks may be dynamically altered in patients with PDM and other chronic pain disorders and that these alterations can be either adaptive or maladaptive^{7,15,16}. Such altered cross-network connectivity and the imbalance between the systems have been suggested to be a

¹Institute of Brain Science, School of Medicine, National Yang-Ming University, Taipei, Taiwan. ²Integrated Brain Research Unit, Division of Clinical Research, Department of Medical Research, Taipei Veterans General Hospital, Taipei, Taiwan. ³Department of Obstetrics and Gynecology, School of Medicine, National Yang-Ming University, Taipei, Taiwan. ⁴Department of Obstetrics and Gynecology, Taipei Veterans General Hospital, Taipei, Taiwan. ⁵Institute of Biomedical Informatics, School of Medicine, National Yang-Ming University, Taipei, Taiwan. *These authors contributed equally to this work. Correspondence and requests for materials should be addressed to L.F.C. (email: lfchen@ym.edu.tw) or J.C.H. (email: jchsieh@ym.edu.tw)

principal pain-related brain abnormality in chronic pain patients¹⁷. The default mode network (DMN) plays an important role in pain disorders^{15,18}. It not only participates in episodic memory and in intrinsic attention but also modulates the experience of pain^{18,19}. The DMN and sensorimotor network (SMN) reorganize in patients with arm amputation that can be with and without phantom pain²⁰. The mPFC, a central node within the DMN, acts as a cardinal coordinator by interacting with the dorsal attention network (DAN), executive control network (ECN) and salience network (SN) during stress and pain adaptation and modulation^{15,21,22}. The ECN balances self-referential awareness with attention to salient information²³ and modulates pain anticipation²⁴. The SN, which is related to anxiety²⁵, is activated when attention is maintained on pain¹⁵. The DAN provides a direct corticocortical pathway for the attentional modulation of pain²². The DMN, ECN and SN networks constitute the core neural systems in the human brain²⁶. To address the resilient crosstalk between these systems under clinical pain condition, PDM as a genuine condition of chronic pain⁷ with spontaneous alternation of painful and pain-free periods may serve as a good clinical model of choice. As pain experiences in females are usually more sophisticated than males²⁷ and PDM subjects are vulnerable to anxiety²⁸, it is plausible the FC alterations in PDMs may be manifested as *trait-related* changes in response to different affective states. Furthermore, PDM may feature functional interactions between large-scale brain networks.

In this study, we implemented a hierarchical approach to study the FC constructs of PDM. We reasoned that FC changes could be manifested as intra-regional (local) and inter-regional (long- distance) FC changes. To study the neuroplasticity of intra-regional FC, we used regional homogeneity (ReHo) analyses to estimate the local synchronization of resting brain activity within a segregated brain region²⁹. An increased local synchrony indicates increased coherence of spontaneous neuronal activity³⁰, which implicates functional integration within a region. Conversely, desynchronized local activity indicates divergent local functions or increased intra-regional functional segregation³¹. To study inter-regional FC alterations among the aforementioned networks, we performed seed-based FC analyses of large-scale networks in the significant regions that were identified in the ReHo analysis. Incorporating ReHo in the seed-based FC analyses may improve the sensitivity of FC analyses and reduce the uncertainty of seed selection³². We considered the regions of ReHo alterations the key functional hubs for PDM, and the changes of inter-regional FCs as seeded on these ReHo-hubs may serve as critical functional correlates for brain resilience under long-term PDM. Collectively, we hypothesized that the local synchronization within hub region(s) of the key systems, particularly the DMN, would be altered and that the functional interactions among the networks (DMN, SN, ECN, and DAN) would be dynamically and functionally reorganized in patients with PDM to cope with the repeated stress of menstrual pain.

Results

Demographic and psychological data. In brief, 46 PDMs and 49 controls (CON) were enrolled in the current neuroimaging study. There were no significant between-group differences regarding age (PDM: 23.33 ± 2.42 years of age, CON: 23.80 ± 2.47 years of age, $p = 0.351$), age at menarche (PDM: 11.93 ± 1.32 years of age, CON: 12.31 ± 1.08 years of age, $p = 0.14$), years of menstruating (PDM: 11.39 ± 2.84 years, CON: 11.49 ± 2.86 , $p = 0.867$), or average duration of one menstrual cycle (PDM: 29.50 ± 1.28 days, CON: 29.52 ± 1.19 days, $p = 0.936$). For the menstrual pain experience, PDM subjects had in average 9.22 ± 2.85 years of pain history; 65.2% of them had absenteeism from school or works and 41.3% of them had taken analgesics occasionally. The PDM group had been experiencing moderate cyclic menstrual pain (present total scores of McGill Pain Questionnaire-pain rating index: 30.11 ± 11.99 , with sensory score: 16.54 ± 6.01 , affective score: 3.91 ± 2.85 , evaluation score: 2.54 ± 2.02 , miscellaneous score: 7.11 ± 3.62 in each category; present pain intensity: 2.72 ± 0.96).

For the psychological inventories, significant group (PDM vs. CON)-phase (menstruation [MENS] vs. periovulatory [POV]) interactions were found in the total ($F = 5.921$, $R^2 = 0.060$, $p = 0.017$) and helplessness scores ($F = 8.498$, $R^2 = 0.084$, $p = 0.004$) of the Pain Catastrophizing Scale (PCS), Beck Anxiety Inventory (BAI; $F = 43.802$, $R^2 = 0.320$, $p < 0.001$), the state anxiety ($F = 20.055$, $R^2 = 0.177$, $p < 0.001$) of Spielberger State-Trait Anxiety Inventory (STAI), and Beck Depression Inventory (BDI; $F = 31.910$, $R^2 = 0.255$, $p < 0.001$). No significant group-phase interactions were found in the rumination ($F = 1.569$, $R^2 = 0.017$, $p = 0.214$) and magnification ($F = 2.021$, $R^2 = 0.021$, $p = 0.158$) scores of the PCS, and trait anxiety of STAI ($F = 2.892$, $R^2 = 0.030$, $p = 0.092$). Significant main effects of group were found in the total ($F = 71.504$, $R^2 = 0.435$, $p < 0.001$), rumination ($F = 75.315$, $R^2 = 0.447$, $p < 0.001$), helplessness ($F = 68.698$, $R^2 = 0.425$, $p < 0.001$) and magnification ($F = 31.026$, $R^2 = 0.250$, $p < 0.001$) scores of the PCS, BAI ($F = 57.994$, $R^2 = 0.384$, $p < 0.001$), the state anxiety ($F = 16.437$, $R^2 = 0.150$, $p < 0.001$) and trait anxiety ($F = 8.312$, $R^2 = 0.083$, $p = 0.005$) of STAI, and BDI ($F = 14.514$, $R^2 = 0.135$, $p < 0.001$). Significant main effects of phase were found in the BAI ($F = 27.334$, $R^2 = 0.227$, $p < 0.001$), state anxiety ($F = 23.071$, $R^2 = 0.199$, $p < 0.001$) of STAI and BDI ($F = 20.724$, $R^2 = 0.182$, $p < 0.001$). No main effects of phase were found in the total ($F = 3.276$, $R^2 = 0.034$, $p = 0.074$), rumination ($F = 2.544$, $R^2 = 0.027$, $p = 0.114$), helplessness ($F = 3.713$, $R^2 = 0.038$, $p = 0.057$) and magnification ($F = 0.264$, $R^2 = 0.003$, $p = 0.609$) scores of the PCS, and the trait anxiety ($F = 1.518$, $R^2 = 0.016$, $p = 0.221$) of STAI (see Supplementary Table S1).

Serum hormone levels. There were no significant between-group differences regarding the levels of estradiol, progesterone or testosterone in MENS phase and POV phase, respectively (see Supplementary Table S2).

Intra-regional connectivity (ReHo). For the interaction effect, the between-group comparison of phase differences revealed significant greater ReHo alterations in the left declive and right orbitofrontal cortex (OFC), and lesser ReHo alterations in the left aIPS/SPL in the PDM group (Table 1; Fig. 1A). No main effects of group and phase were noted. For the between-group planned contrast, there was no difference during the MENS phase. The bilateral ventromedial prefrontal cortex (vmPFC, BA10) of DMN network, exhibited a trait-related reduction of ReHo during the POV phase in the PDM group vs. CON group (Table 1; Figs 1A and S1). For the between-phase

Contrast	Region	BA	Size	t_{score}	Coordinate		
					x	y	z
Main effects of group (PDM vs. CON)							
PDM > CON	NS						
CON > PDM	NS						
Main effects of phase (MENS vs. POV)							
MENS > POV	NS						
POV > MENS	NS						
Interaction							
PDM _{Δ(MENS-POV)} > CON _{Δ(MENS-POV)}	declive	–	415	4.62	–22	–68	–26
	OFC	10	512	3.94	38	52	–12
CON _{Δ(MENS-POV)} > PDM _{Δ(MENS-POV)}	aIPS/SPL	40	429	4.58	–42	–38	52
Between-group planned contrast							
MENS: PDM > CON	NS						
MENS: CON > PDM	NS						
POV: PDM > CON	NS						
POV: CON > PDM	vmPFC	10	377	3.89	6	62	22
				3.6	0	66	12
				3.51	–6	50	4
Between-phase planned contrast							
PDM: MENS > POV	NS						
PDM: POV > MENS	aIPS/SPL/VPL	40	520	5.11	–42	–36	48
				3.5	–30	–26	44
				3.39	–36	–46	56
CON: MENS > POV	NS						
CON: POV > MENS	declive	–	409	5.22	–22	–68	–26

Table 1. The main effect of group and phase, interaction effect, between-group differences, and within-group differences in regional homogeneity. Peak coordinates refer to Montreal Neurological Institute space. Significance was set at the uncorrected voxel level $p = 0.005$ followed by the FWE-corrected cluster level $p = 0.05$. BA, Brodmann area; OFC, orbitofrontal cortex; vmPFC, ventromedial prefrontal cortex; VPL, ventral parietal lobe; aIPS, anterior part of the intraparietal sulcus; SPL, superior parietal lobe; MENS, menstruation phase; POV, periovulatory phase; PDM, primary dysmenorrhea group; CON, control group; NS, non-significant.

planned contrast, PDM group demonstrated *state-related* reduction of the ReHo in the anterior part of the left intraparietal sulcus (aIPS, BA40) and left superior parietal lobe (SPL) of DAN network during the MENS phase vs. the POV phase (Table 1; Figs 2A and S1). The CON group demonstrated *state-related* reduction of ReHo in the left declive during the MENS phase vs. the POV phase.

Inter-regional connectivity (FC). *vmPFC (DMN network).* For the interaction effect, the PDM group as compared to the CON group exhibited greater left vmPFC ($x = -6, y = 50, z = 4$)-supplementary motor area (SMA) FC during MENS phase relative to POV phase (Table 2; Fig. 1B). No interaction was found when the right vmPFC ($x = 6, y = 62, z = 22$) was used as the seed. For the main effects, please refer to the Supplementary Table S3. For the between-group planned contrast, the PDM group as compared to the CON group exhibited hypoconnectivity of the left vmPFC-bilateral dorsal anterior cingulate cortex (dACC; substrate of SN network) circuit and hyperconnectivity of the left vmPFC-left dorsomedial prefrontal cortex (dmPFC; substrate of ECN network) circuit during both phases. In addition, the PDM group as compared to the CON group exhibited hypoconnectivity of the left vmPFC-bilateral pregenual anterior cingulate cortex (pACC; substrate of SN network) circuit and hyperconnectivity of the left vmPFC-left dorsolateral prefrontal cortex (DLPFC; substrate of ECN network) and left ventral parietal lobe (VPL; substrate of ECN network) circuits during the POV phase (Fig. 1B; Table 2; Figs S2, S3). Furthermore, both the right vmPFC-right inferior frontal gyrus (IFG; substrate of SN network) circuit and the right vmPFC-pACC circuit (DMN-DMN network) exhibited hypoconnectivity in the PDM group as compared to CON group during the POV phase (Table 2; Fig. S4). No between-group difference was detected during the MENS phase when the right vmPFC was used as the seed. For the between-phase planned contrast, no difference was found in the PDM group when the left vmPFC was seeded. In the CON group, hypoconnectivity of the left vmPFC-SMA circuit was found during the MENS phase as compared to the POV phase. In the PDM group, hypoconnectivity of the right vmPFC-pons circuit was found during the MENS phase as compared to the POV phase (Table 2). There was no between-phase difference in the CON group when the right vmPFC was seeded.

aIPS/SPL (DAN network). For the interaction effect, no group-phase interaction was found when the left aIPS/SPL ($x = -42, y = -36, z = 48$) was seeded. For the main effects, please refer to the Supplementary Table S4. For the between-group planned contrast, the PDM group as compared to the CON group exhibited hyperconnectivity

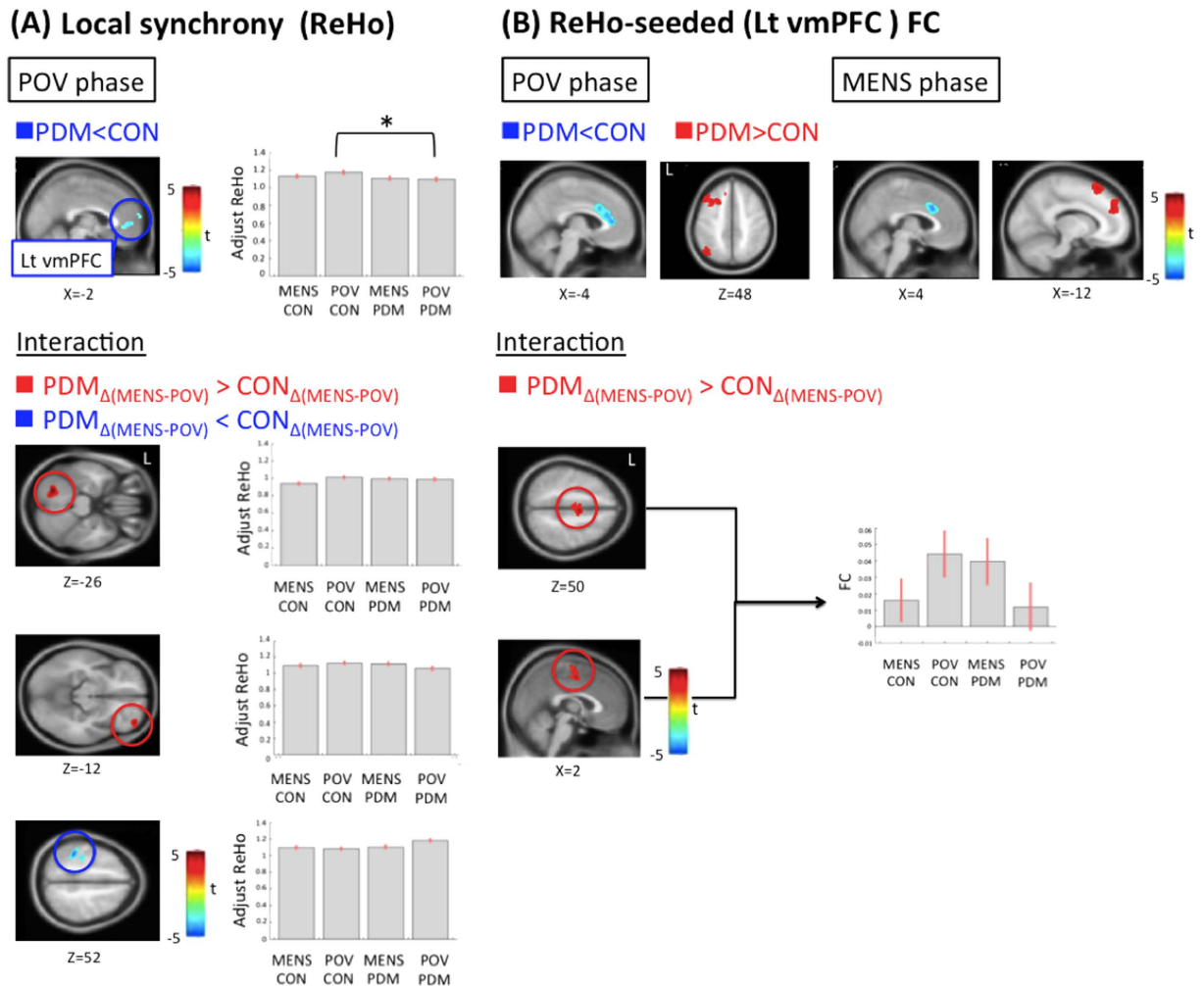


Figure 1. Statistical maps of ReHo, ReHo-seeded (Lt vmPFC) FC and the interaction effects. (A) *ReHo* maps. PDM group shows decreased ReHo of the Lt vmPFC during the POV phase when comparing to the CON group. For the interaction effect, the between-group (PDM vs. CON) comparison of phase differences (MENS vs. POV) reveals significant greater ReHo alterations in the Lt declive and right orbitofrontal cortex (OFC), and lesser ReHo alterations in the Lt anterior intraparietal sulcus and superior parietal lobule. The bar charts show adjusted ReHo values at the peak voxel of the vmPFC. The error bar corresponds to a 90% confidence interval. (B) *FC* maps. For ReHo-seeded (Lt vmPFC) FC between-group comparisons, hypoconnectivity in the Lt vmPFC-dorsal anterior cingulate cortex FC and hyperconnectivity in the Lt vmPFC-dorsomedial prefrontal cortex FC are noted in the PDM group when compared to the CON group during both phases. Hypoconnectivity in the Lt vmPFC-pregenual anterior cingulate cortex FC and hyperconnectivity in the Lt vmPFC-dorsolateral prefrontal cortex and -ventral parietal lobe FCs are observed in the PDM group during the POV phase. The PDM group (vs. CON group) shows greater between-phase (MENS vs. POV) Lt vmPFC-supplementary motor area (SMA) FC. Red regions are associated with increased FC and greater phase-difference of ReHo or FC in the PDM group. Blue regions are associated with decreased ReHo, decreased FC and lesser phase-difference of ReHo or FC in the PDM group. Significance thresholded at the uncorrected voxel level $p = 0.005$ followed by the FWE-corrected cluster level $p = 0.05$. ReHo, regional homogeneity; PDM, primary dysmenorrhea; CON, control; MENS, menstrual phase; POV, periovulatory phase; FC, functional connectivity; vmPFC, ventromedial prefrontal cortex; Lt, left. *Denotes the contrast(s) that are significant in between-group comparisons.

of the aIPS/SPL-MTG circuit and hypoconnectivity of the aIPS/SPL-anterior lobe of the cerebellum circuit during the MENS phase. The PDM group as compared to the CON group exhibited hyperconnectivity of the aIPS/SPL-MTG and -middle occipital gyrus circuits during the POV phase. For the between-phase planned contrast, PDM group exhibited hypoconnectivity of the aIPS-bilateral posterior insula (DAN-pain matrix) and -right postcentral gyrus circuits (DAN-pain matrix) during the MENS phase as compared to the POV phase (Fig. 2B; Table 3). No significant between-phase difference was found in the CON group.

Correlation between FC and psychological measurements. In the PDM group, the FC of the left vmPFC-bilateral posterior-mid insula (DMN-pain matrix connectivity) and -dACC (DMN-pain matrix connectivity) were more

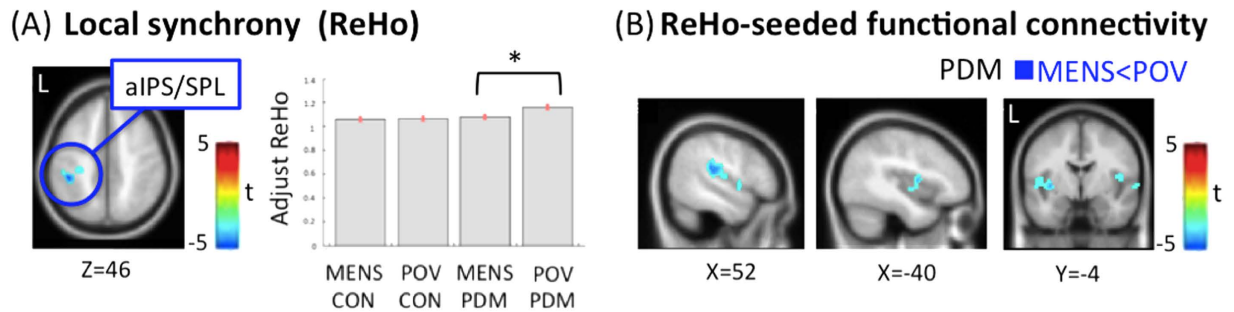


Figure 2. The state-related ReHo and FC alterations in PDM. (A) *ReHo maps*. PDM group shows decreased ReHo of the anterior part of the intraparietal sulcus (aIPS) and superior parietal lobe (SPL) during the MENS phase when compared to the POV phase. The bar charts indicate the adjusted ReHo values at the peak voxel of the aIPS/SPL. The error bar corresponds to a 90% confidence interval. (B) *FC maps*. For ReHo-seeded (aIPS/SPL) FC between-phase comparisons, hypoconnectivity in the aIPS-bilateral posterior insula and -right postcentral gyrus FCs are observed during the MENS phase in the PDM group. Blue regions are associated with either decreased ReHo or decreased FC. Significance thresholded at the uncorrected voxel level $p = 0.005$ followed by the FWE-corrected cluster level $p = 0.05$. *Denotes the contrast(s) that are significant in between-phase comparisons. For abbreviations, see the legend of Fig. 1.

Contrast	Region	BA	Size	t_{score}	Coordinate		
					x	y	z
left side ReHo-seed (-6, 50, 4)							
Interaction							
$PDM_{\Delta(MENS-POV)} > CON_{\Delta(MENS-POV)}$	SMA/MCC	6	539	3.95	2	-6	50
Between-group planned contrast							
MENS: PDM > CON	SFG	6	388	3.97	-14	24	58
	dmPFC	9	384	3.94	-10	48	28
MENS: CON > PDM	dACC	32	374	4.2	2	20	32
POV: PDM > CON	dmPFC/DLPFC	8	952	4.24	-12	30	40
	VPL/angular	39	372	3.85	-42	-68	48
POV: CON > PDM	pACC	24	823	4.28	0	38	10
					2	22	28*
Between-phase planned contrast							
CON: POV > MENS	SMA	6	580	4.46	-12	-12	54
right side ReHo-seed (6, 62, 22)							
Between-group planned contrast							
POV: CON > PDM	IFG	-	335	5.06	46	20	6
	pACC	32	691	3.99	4	40	8
Between-phase planned contrast							
PDM: POV > MENS	pons	-	325	4.58	12	-38	-34

Table 2. Significant interaction effect, between-group and within-group differences in ReHo-seed (vmPFC) functional connectivity analyses. Peak coordinates refer to Montreal Neurological Institute space. Significance thresholded at the uncorrected voxel level $p = 0.005$ followed by the FWE-corrected cluster level $p = 0.05$. SMA, supplementary motor area; MCC, midcingulate cortex; SFG, superior frontal gyrus; dmPFC, dorsomedial prefrontal cortex; dACC, dorsal anterior cingulate cortex; DLPFC, dorsolateral prefrontal cortex; VPL, ventral parietal lobe; pACC, pregenual anterior cingulate cortex; IFG, inferior frontal gyrus (see Table 1 for other abbreviation details) *the second highest peak, almost the same location with the highest peak in the MENS phase.

correlated with BAI during the POV phase when compared to the MENS phase (Fig. 3; Table 4). The FCs of the left vmPFC-bilateral midcingulate cortex and -right middle frontal gyrus positively correlated with BAI, and the FC of the left vmPFC-bilateral declive negatively correlated with BAI during the POV phase. The FC of the right vmPFC-right inferior temporal gyrus and -left declive circuit negatively correlated with BAI during the POV phase. The FCs of the aIPS-bilateral rectal gyrus and -right cerebellum connectivity and BAI were significantly more correlated during the POV phase when compared with the MENS phase. The FC of the aIPS-bilateral rectal gyrus positively correlated with BAI and the FC of the aIPS-left precuneus negatively correlated with BAI during the POV phase. For brain-behavioral correlations, there was no significant correlation during the MENS phase (Table 4).

Contrast	Region	BA	Size	t_{score}	Coordinate		
					x	y	z
Between-group planned contrast							
MENS: PDM > CON	MTG	39	323	3.71	40	-60	20
MENS: CON > PDM	cerebellum anterior lobe	31	378	4.34	6	-48	-34
POV: PDM > CON	STG/MTG	22	996	4.54	56	-56	6
	MOG	19	469	4.27	-34	-80	-2
Between-phase planned contrast							
PDM: POV > MENS	claustrum	-	351	4.01	-36	-8	0
	supramarginal	40	498	4.35	54	-26	18
	insula	13	434	4.16	42	2	6

Table 3. Significant between-group and within-group differences in ReHo-seed (aIPS/SPL) functional connectivity analyses. Peak coordinates refer to Montreal Neurological Institute space. Significance was set at the uncorrected voxel level $p = 0.005$ followed by the FWE-corrected cluster level $p = 0.05$. MTG, middle temporal gyrus; STG, superior temporal gyrus; MOG, middle occipital gyrus.

Discussion

Using ReHo and ReHo-seeded FC analyses, the current study demonstrated *state-* and *trait-related* intra- and inter-regional FC alterations that collectively may result in subclinical central modulations of pain in otherwise healthy women with PDM. In our study, we observed a decreased ReHo, or a reduced local synchrony, in the vmPFC, which indicates increased intra-regional functional segregations in reaction to long-term menstrual pain. We also measured changes of inter-regional FC (both intrinsic and extrinsic network connectivity) in the PDM group, which may represent network reorganization in the context of strengthened DMN-ECN FC and attenuated DMN-SN FC when compared to the CON group. In addition, functional interaction between aIPS/SPL and pain-related regions (DAN-pain matrix connectivity) might be associated with a top-down regulation of pain transmission. Finally, we observed an inverse correlation between the vmPFC-posterior/mid insula FC (DMN-pain matrix connectivity) and anxiety scores across different phases. This suggests an adaptive neuroplasticity that is related to pain-primed mental state changes.

The vmPFC of PDM group manifested a relative lack of resilience (Fig. 1A) across the menstrual cycle as reflected in the significantly lower ReHo in the PDMs vs. CONs. The functional expression of DMN throughout the menstrual cycle differed between PDM and CON groups. The stereotyped desynchronized local activity (similar ReHo value across the menstrual cycle) in the PDMs indicates sustained and constrained neuroplasticity for divergent local functionalities or enhanced intra-regional functional segregation³¹. Being a part of the DMN and a functional hub of the brain, the vmPFC integrates and regulates conceptual information, including affective sensory, self-perception, social cognition, and emotion^{10,33}. The vmPFC is also involved in the anticipatory coping mechanism³⁴. It has also been suggested that the vmPFC and the linked nucleus accumbens constitute a system that mediates the effects of self-regulation on pain evaluation^{14,35}. Of note, the DMN is a key network altered in chronic pain diseases¹⁷ and abnormal resting-state FC of it can be associated with pain intensity and rumination³⁶⁻³⁸. The ReHo reduction herein could possibly be attributed to various factors, such as the self-regulation of emotion, behavioral coping, appraisal/re-appraisal of self-relevant social information, and adaptation for pain modulation in relevant networks in response to PDM.

The functional expression and engagement of DAN throughout the menstrual cycle differed between PDM and CON groups, as reflected by the interaction effect of group and phase. The aIPS/SPL services attention shifting and saliently driven sensory discrimination and is a cardinal substrate of the DAN that participates in the top-down attention to pain²². Therefore, the relative lower ReHo of aIPS/SPL during the MENS phase vs. the POV phase in the PDM group (Figs 1A and 2A) might implicate an active disengagement of pain attention as part of salience modulation. The relative higher ReHo of the aIPS/SPL during the POV phase might connote an overt integration of the functionality for salience detection for the forthcoming stressful events.

Greater ReHo (MENS vs. POV) of the declive and the orbitofrontal cortex (OFC) in the PDM as compared to the CON group (Fig. 1A) could be adaptive to long-term menstrual pain. The OFC plays an important role in visceral sensory/nociceptive processing, and is activated during MENS phase of PDMs⁶. The OFC is crucial to adaptively cope with physiological challenges, regulate affective states and modulate pain³⁹. Of note, we also found greater left vmPFC-SMA FC during MEMS (vs. POV phase) in PDM group as compared to CON group (Fig. 1B). The medial brain motor area has been suggested to be a visceromotor area and has underrecognized modulatory influence on visceral processes⁴⁰. In addition, many chronic pain conditions are associated with increased DMN-SMN (including SMA) FC^{17,20}. The group-phase interaction of vmPFC-SMA FC (DMN-SMN network) indicates that the cross-network communication is altered in the PDM group. Similar to our recent finding of periaqueductal gray matter (PAG) FC changes to the DMN⁷, the altered DMN-SMN network may be an ongoing representation of cumulative menstrual pain, which might be generated in part by FC dysfunction between medial brain motor regions and both DMN and PAG⁴⁰.

The functional interplay between the three core networks might reorganize after stress events⁴¹. In the present study, we observed reduced connectivity in the vmPFC-dACC circuit (DMN-SN network) in the PDM group. The dACC is a critical neural substrate of the SN network⁴². Hong *et al.*⁴³ suggested that females allocate more neural resources to interoceptive awareness. The authors demonstrated hypoconnectivity between the SN- and

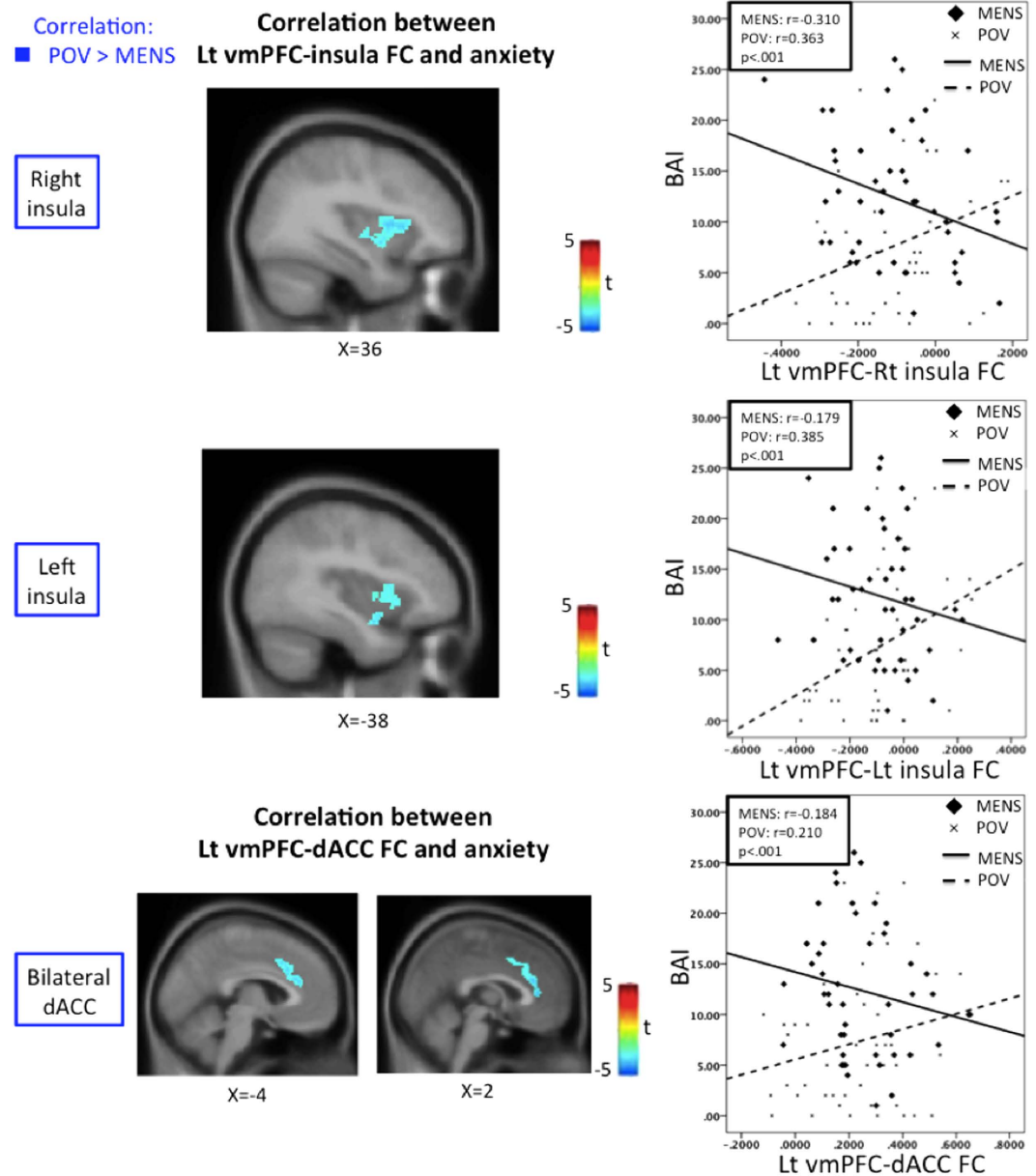


Figure 3. Correlation between FC and anxiety score inverses across phases in PDM. The Lt vmPFC-Rt insula, -Lt insula and -bilateral dorsal anterior cingulate cortex (dACC) FCs are positively correlated with BAI during the POV phase but negatively correlated with BAI during the MENS phase. Original FC values were used for the correlation to avoid artificial and inadvertent zeroing. Blue regions are associated with lower correlation with BAI during MENS phase. Significance thresholded at the uncorrected voxel level $p = 0.005$ followed by the FWE-corrected cluster level $p = 0.05$. BAI, Beck Anxiety Inventory; Lt, left; Rt, right.

DMN-related regions in patients with irritable bowel syndrome (a chronic pain condition that is often comorbid with PDM). Such reduced DMN-SN FC can be adaptive for stress and anxiety⁴⁴ and perhaps a reactive modulation to PDM. Conversely, we found hyperconnectivity in the vmPFC-VPL (DMN-ECN network) and vmPFC-DLPFC circuits (DMN-ECN network) in the PDM group. These two regions of the ECN are associated with pain attention and modulation^{22,45}. The dynamic transition from the DMN-SN to DMN-ECN FC in individuals with PDM might implicate a shift from affective processing of pain salience to the cognitive modulation of long-term menstrual pain. DMN engagement is essential to an improved performance in self-related tasks⁴⁶, including the reappraisal (involving both ECN and DMN⁴⁷) of potentially harmful inputs that can intervene relatively early in the process of emotion-generation and the recruitment of executive cognitive control processes. This cross-network coordination plausibly implicates a functional plasticity and a coping mechanism underlying a normal protective adaptation in females with PDM as a result of repeated cyclic stress.

The right anterior insula and right inferior frontal gyrus exhibited *trait-related* decrease of FC with right vmPFC (Fig. S4, Table 2), and are involved in the SN and right-lateralized ventral attention network (VAN),

ReHo-seed	Positive correlation							Negative correlation								
	Region	BA	Size	t_{score}	Coordinate			Region	BA	Size	t_{score}	Coordinate				
					X	Y	Z					X	Y	Z		
left vmPFC (-6, 50, 4)																
POV																
	MFG	10	388	4.69	28	48	12	declive	-	265	3.99	-12	-68	-22		
	MCC	24	354	4.04	2	2	38									
MENS > POV																
	NS							insula/dACC	-	1292	4.84	36	-10	-2		
											4.04	-6	22	26		
											3.82	2	36	8		
								insula	-	618	4.26	-28	4	14		
right vmPFC (6, 62, 22)																
POV																
	NS							ITG	21	273	4.34	58	-10	-18		
								declive	-	431	3.9	-10	-74	-28		
aIPS/SPL (-42, -36, 48)																
POV																
	rectal gyrus	11	536	5.09	-4	28	-26	precuneus/ postcentral gyrus	5/7	874	4.76	-6	-50	66		
MENS > POV																
	NS							rectal gyrus	11	803	5	4	18	-26		
								cerebellum	-	351	4.59	50	-70	-36		

Table 4. ReHo-seeded functional connectivity significantly covarying with the Beck Anxiety Index (BAI). Peak coordinates refer to Montreal Neurological Institute space. Significance was set at the uncorrected voxel level $p = 0.005$ followed by the FWE-corrected cluster level $p = 0.05$. MFG, middle frontal gyrus; MCC, midcingulate cortex; ITG, inferior temporal gyrus; dACC, dorsal anterior cingulate cortex; NS, non-significant. (see Table 1 for other abbreviation details).

respectively; possibly encoding the prolonged salience of pain⁴⁸. The hypoconnectivity might connote a possible coping in active inhibition of interoceptive awareness for pain saliency and attention to pain. The hypoconnectivity of the aIPS-right postcentral gyrus and -bilateral posterior-mid insula FCs (DAN-pain matrix connectivity) can also be adaptive in patients with chronic PDM. The postcentral gyrus and posterior-mid insula service the discriminative dimension of pain experience^{49,50}. The posterior insula integrates viscerosensory and motor processing, and participate in the interaction between motor cortical areas controlling painful body regions and distant non-motor cortical brain regions⁵¹. As a neural substrate of the DAN, the aIPS/SPL has an important role in top-down attention regulation⁵², which modulates pain perception²². Diverting attention from pain can decrease the activity of the ascending pain system⁵³ and can be mechanistic for cognitive-behavioral therapy and meditation⁵⁴. Grant *et al.*⁵⁵ reported that meditators who are less sensitive to pain feature a decoupled FC between the dACC and the dorsolateral prefrontal cortex. This disengagement from higher-order evaluative processes has an important role in the regulation of pain and emotion as well as in cognitive control⁵³.

As a part of the pain matrix⁵⁰, the insula integrates interoception into the subjective social-emotion⁵⁶ and has an important role in allocating attention and evaluating context^{57,58}. Beside, dACC and mPFC are associated with interoceptive awareness, and play an important role in the appraisal and expression of fear and anxiety¹⁰. Increased DMN/mPFC-insula FC has been reported in several chronic pain disorders^{18,37}. The alteration of mPFC-insula FC is also present in the unpleasant itch condition⁵⁹. Chronic pain and itch may invoke guarding or scratching behaviors and elicit anxiety concomitantly. Hence, the mPFC-insula FC could be a state-specific biomarker for chronic pain perception³⁸. This proposition has been corroborated by a study that found that opioids exert their analgesic efficacy by disrupting the vmPFC/rACC-insula FC⁶⁰. State anxiety is positively correlated with DMN-insula FC in healthy subjects⁶¹. Although pain and anxiety are based on distinguishable neural mechanisms⁶², anxiety is often accompanied by menstrual pain^{3,5,6}. In the present study, a trend of positive correlation between mPFC-posterior-mid insula FC (DMN-pain matrix connectivity) and anxiety was observed during the POV phase. This finding is consistent with the view that neuroticism can be a personality trait in patients with PDM⁶³. The positive correlation shifted to a negative correlation when menstrual pain was present, thereby implicating a possible adaptation to pain-primed anxiety.

Pain is a subjective experience with wide individual differences. One possible explanation is that females with PDM have a propensity for anxiety that can be attributed to genetic factors, such as the *BDNF* Val66Met polymorphism³. *BDNF* genotypes may exhibit cognitive and neurobiological differences⁶⁴. In addition, menstrual pain is accompanied by complex and subtle changes in emotion and cognition. The associated coping strategies and emotional and cognitive regulation vary across individuals. It can be heuristic to explore the interaction between the *BDNF* Val66Met polymorphism and its neuronal regulation to stress in individuals with PDM.

The neuroimaging is a sensitive measurement that can provide subclinical or preclinical evidence of significant alterations in brain function even without conspicuous behavioral manifestations⁶⁵. Our results suggest

that PDM subjects, after long-term cyclic menstrual pain, may develop neuroplasticity and brain reorganization as manifested by intra- and inter-regional FC changes (intrinsic and extrinsic network connectivity) of neural networks. The interoceptive awareness and switching roles of the SN network for pain saliency can be substituted by cognitive control function of the ECN network. Such resilient transition can be adaptive in long-term PDM subjects and may contribute to the understanding of system dynamics of functional pain connectome in other acute and chronic pain conditions¹⁵.

Materials and Methods

Subjects. The subjects of this study were a subset of the participants from our previous genetic association and behavioral studies of PDM who were eligible for neuroimaging studies³. Originally, 326 PDMs and 209 CONs were registered during August 2011 to March 2014 as intended for the integrated behavioral and multimodal imaging genetics studies (magnetic resonance imaging and magnetoencephalography). Two hundred and twenty-nine PDMs and 103 CONs were then excluded after rigorous screening according to the exclusion criteria and one or a combination of the following factors: an irregular menstrual cycle, a prolonged or shortened menstrual cycle, inconsistent pain intensity, pelvic abnormalities by ultrasonography as examined after entering the program, or being unwilling to complete the entire series of genetic, hormonal, behavioral, and multimodal neuroimaging studies (see also Lee *et al.*³). After entering the actual multimodal neuroimaging experiments, 11 PDMs and 3 CONs were excluded due to incidental brain findings (see also Li *et al.*²); 36 PDMs and 38 CONs excluded from subsequent analyses due to drop-out that ended in incomplete dataset; 2 PDMs and 10 CONs excluded owing to abnormal hormone level (possibly due to sampling and technical errors); and 2 PDMs and 6 CONs excluded owing to the head motion (>2 mm) or rotation (>2°) during the scan. Eventually, 46 PDMs and 49 CONs were eligible for neuroimaging analyses in this study (whole protocols completed), as also reported in our recently published functional connectivity study of PDM (see Wei *et al.*⁷).

The inclusion criteria for subjects with PDM included: 1) 20–30-year-old Taiwanese (Asian) females; 2) a regular menstrual cycle of approximately 27–32 days; 3) a history of menstrual pain longer than 6 months; 4) averaged menstrual pain under regular treatment with a rating at least higher than 4 on a verbal numerical scale (VNS, 0 = not at all, 10 = the worst imaginable pain) in the last 6 months; and 5) right-handedness, as confirmed by the Edinburgh Handedness Inventory. All subjects in the PDM group underwent pelvic ultrasonography to exclude secondary dysmenorrhea that was caused by organic pelvic diseases, such as endometriosis or adenomyosis. All participants were clinically examined and diagnosed in the gynecology clinic by the same gynecologist. The inclusion criteria for the healthy female control subjects were similar to those for the PDM group, with the exception that the members of the control group must have no pain during menses (VNS = 0). The exclusion criteria for all the participants were: 1) using oral contraceptives, hormonal supplements, Chinese herbal medicine, or any central-acting medication (e.g., opioid, anti-epileptics) within 6 months prior to the study; 2) pathological pituitary gland disease; 3) organic pelvic disease; 4) any psychiatric or neurological disorders; 5) brain trauma or brain surgery; 6) immediate plans for pregnancy or a positive pregnancy test; 7) a history of childbirth; and 8) having a metal/pacemaker implant, claustrophobia, or any contraindications to magnetic resonance imaging (MRI). No analgesics were used within 24 hours of the scans. The study was conducted in accordance with the Declaration of Helsinki and was approved by the Institutional Review Board of Taipei Veterans General Hospital. Written informed consents were obtained from all participants.

Experimental design. MRI scanning was individually scheduled according to the commencement day of menstruation for each subject. Psychological assessments, blood samples for gonadal hormone assays and MRI images (T1 and resting-state fMRI images) were obtained at two time points during the menstrual cycle: the MENS phase (days 1–3 of the menstrual cycle) and the POV phase (days 12–16 of the menstrual cycle). Ovulation was confirmed using a urinary luteinizing hormone test (Han Chiun Proper LH Rapid Test).

Psychological measurements. The patients in the PDM group completed the PCS and recounted their overall menstrual pain by using the McGill Pain Questionnaire during the inception interview. Then, during the MENS phase, subjects were assessed for their present experience of menstrual pain using the McGill Pain Questionnaire. All participants completed the BDI, BAI and STAI during the MENS and POV phases to assess their psychological status.

Serum gonadal hormone measurements. The serum that was extracted during both phases was stored for batch analysis using commercialized assays (UniCel DxC 800 Synchron Clinical Systems, Beckman Coulter, Inc., Brea, CA). The total serum concentrations were assayed using a chemiluminescence immunoassay technique for estradiol and progesterone and a radioimmunoassay technique for the testosterone. As gonadal hormones may affect resting-state FC⁶⁶, hormone fluctuations were regressed out as covariates of non-interest in the following image processing.

Image acquisition. Resting-state functional MRI images were acquired using a 3.0 Tesla MRI scanner (Magnetom Trio Tim, Siemens, Erlangen, Germany) with a 12-channel head coil. High-resolution T1-weighted 3-dimensional structural images using a magnetization-prepared rapid-acquired gradient echo sequence (MPRAGE; [TR]/[TE] = 2530 ms/3.03 ms, flip angle = 70°, field-of-view = 224 × 256 × 192 mm³, in-plane matrix size = 224 × 256 × 192, in-plane resolution = 1 mm) and T2*-weighted gradient echo sequence ([TR]/[TE] = 2500 ms/30 ms, flip angle = 90°, field-of-view = 220 × 220 × 136 mm³, in-plane matrix size = 64 × 64 × 40, in-plane resolution = 3.4 mm [round-out], and 204 volumes per run) were conducted to obtain high-resolution anatomical T1 images and functional MRI images. The first four functional scans of each resting-state functional MRI series were discarded for signal saturation and magnetic field stabilization. Participants remained awake during the scan and were instructed to maintain open eyes and relaxed, still heads without thinking about any topic in particular. Head cushions and earplugs were applied to reduce head motion and noise.

Resting-state analysis. *Regional homogeneity (ReHo) analysis.* Preprocessing was performed by using the Data Processing Assistant for Resting-State fMRI (DPARSF) V2.3 Advanced Edition (State Key Laboratory of Cognitive Neuroscience and Learning, Beijing Normal University, China)⁶⁷ with statistical parametrical mapping 8 (SPM 8; Wellcome Trust Center for Neuro-imaging, University College London, London, UK) in Matlab 2013b (The MathWorks, Inc., Natick, MA, USA). The preprocessing protocol was adapted from previous studies⁶⁸. In brief, all functional images were slice-time corrected and realigned for head motion correction. Subjects with head motion of any volume more than 2 mm or 2° were excluded from further processing. Images were normalized using the SPM's standard echo planar imaging template in Montreal Neurological Institute (MNI) space and re-sampled to an isotropic 2 mm³ voxel size. The resulting time series in each voxel was then linearly detrended and band-pass filtered (0.01–0.08 Hz) to extract the low-frequency oscillations. The following nuisance variables were regressed out: 1) the six head movement parameters computed based on rigid body translation and rotation during the realignment in SPM8; 2) the mean signal within the lateral ventricles for cerebral spinal fluid; and 3) the mean signal within a deep white matter region (centrum ovale). Brain activity was activated in clusters, or contiguous voxels, rather than in a few voxels. ReHo maps were generated by calculating the Kendall's coefficient of concordance (KCC) of the time series between a given voxel with its nearest neighbors (26 voxels) in a voxel-wise manner. The ReHo maps were spatially smoothed using a 3D Gaussian kernel of 6 mm full-width at half-maximum (FWHM). For standardization purposes, each individual subject's ReHo map was divided by its own global mean. The peaks of significant clusters were then selected as the ReHo-based seeds.

Functional connectivity analysis of ReHo-based seeds. The preprocessing of the functional connectivity analysis protocol was as same as in the ReHo analysis, except that the images were 1) coregistered to individuals' anatomical image and then normalized to the standard T1 MNI template; 2) spatially smoothed using a 3D Gaussian kernel of 8 mm FWHM; and 3) treated with the global mean signal for additional nuisance variables. We performed global signal regression because it has been shown to maximize the specificity of positive resting-state correlations when using real and simulated data⁶⁹. However, the neuroscientific interpretation of anti-correlation has been challenged⁷⁰, and global signal regression may cause a negative shift in the distribution of correlations^{71,72}; therefore, we implemented a mask and addressed positive connectivity only⁷. The seeded regions that were selected for FC analysis were those wherein the ReHo significantly differed in the between-group and between-phase comparisons. The mean time series activity was extracted within the 3mm radius spherical ReHo-seeded regions. There is no strict universal standard or any fixed parameter for the seed definition in various modalities of neuroimaging. We had used 3 mm as the radius for the seeds in our published functional studies^{7,73}. Three-mm was chosen out of the concern to avoid additional partial volume effect since our original fMRI resolution is 3.4 × 3.4 × 3.4 mm and the cortical thickness as reported is about 2 to 4 mm across the brain⁷⁴. The individual FC maps were computed by the Pearson's correlation coefficient (r) between the seeds and the related brain regions. After calculating the correlation between the reference time course and the time course of each voxel in the brain, r values were converted into z -values using Fisher's r -to- z transformation to normalize the distribution. Finally, we only used positive FC maps in subsequent analyses to minimize the possible influences of artifacts of anticorrelations.

Network assignments for the altered ReHo and FC regions. For the network assignments for the significantly altered ReHo and FC regions, we conducted the inverse validation by means of FC analyses, using peaks of significant clusters as the seeds. The FC was considered significant if family-wise error level was $p < 0.05$ at voxel level. The FC map of each seed was visually compared with the FC map of the key brain systems as published previously⁷⁵. Basically, all the reported network assignments were affirmed by this procedure.

Statistical analyses. *Demographic and psychological data.* SPSS Statistics 20.0 (SPSS Inc., Chicago, IL) was used for all analyses. Two-sample t -tests were conducted for the between-group (PDM vs. CON) differences in demographic characteristics and Edinburgh Handedness Inventory scores. To test the group-phase interactions, we used mixed design two-way ANOVA. The significance was thresholded at $p = 0.05$. For more comprehensive statistical analyses and results, please refer to our previous paper by Lee *et al.*³.

Image data: ReHo and ReHo-seeded FC. For the interaction effects of group and phase, we compared the phase difference (MENS phase vs. POV phase) of mean ReHo values and ReHo-seeded FCs between the PDM and CON groups by the factorial design module of SPM8. To elucidate the respective *trait*- and *state*-related neuroplasticity, we focused on the planned contrasts of between-group differences of respective phase and between-phase differences of respective group rather than the main effects for ReHo values and ReHo-seeded FCs^{5,7}. The planned between-group and between-phase comparisons of imaging data were conducted using 2-sample and paired t test, respectively. Main effects analyses were also conducted for reference only. Three gonadal hormone levels were treated as non-interest covariates. Significance was thresholded at the uncorrected voxel level $p = 0.005$ followed by the FWE-corrected cluster level $p = 0.05$.

Image data: brain-behavior correlation. Since studies have reported that state anxiety correlate with mPFC-insula FC⁶¹, we also applied regression analyses between ReHo-seeded FC and BAI for the PDM group. Three gonadal hormone levels were treated as non-interest covariates. Significance was thresholded at the uncorrected voxel level $p = 0.005$ followed by the FWE-corrected cluster level $p = 0.05$.

References

- Berkley, K. J. Primary Dysmenorrhea: An Urgent Mandate. *Pain: Clinical Updates* **21**(3), 1–8 (2013).
- Li, W. C. *et al.* High prevalence of incidental brain findings in primary dysmenorrhoea. *Eur J Pain* **19**, 1071–1074 (2015).
- Lee, L. C. *et al.* Association of brain-derived neurotrophic factor gene Val66Met polymorphism with primary dysmenorrhea. *PLoS One* **9**, e112766 (2014).
- Tu, C. H. *et al.* Brain morphological changes associated with cyclic menstrual pain. *Pain* **150**, 462–468 (2010).
- Tu, C. H. *et al.* Menstrual pain is associated with rapid structural alterations in the brain. *Pain* **154**, 1718–1724 (2013).
- Tu, C. H. *et al.* Abnormal cerebral metabolism during menstrual pain in primary dysmenorrhea. *NeuroImage* **47**, 28–35 (2009).
- Wei, S. Y. *et al.* Changes in functional connectivity of pain modulatory systems in women with primary dysmenorrhea. *Pain* **157**, 92–102 (2016).
- Vincent, K. *et al.* Dysmenorrhoea is associated with central changes in otherwise healthy women. *Pain* **152**, 1966–1975 (2011).
- Melzack, R. Phantom limbs and the concept of a neuromatrix. *Trends Neurosci.* **13**, 88–92 (1990).
- Etkin, A., Egner, T. & Kalisch, R. Emotional processing in anterior cingulate and medial prefrontal cortex. *Trends Cogn Sci.* **15**, 85–93 (2011).
- Rudorf, S. & Hare, T. A. Interactions between dorsolateral and ventromedial prefrontal cortex underlie context-dependent stimulus valuation in goal-directed choice. *J Neurosci.* **34**, 15988–15996 (2014).
- Maren, S., Phan, K. L. & Liberzon, I. The contextual brain: implications for fear conditioning, extinction and psychopathology. *Nat Rev Neurosci.* **14**, 417–428 (2013).
- Tracey, I. Getting the pain you expect: mechanisms of placebo, nocebo and reappraisal effects in humans. *Nat Med.* **16**, 1277–1283 (2010).
- Lee, M. *et al.* Activation of corticostriatal circuitry relieves chronic neuropathic pain. *J Neurosci.* **35**, 5247–5259 (2015).
- Kucyi, A. & Davis, K. D. The dynamic pain connectome. *Trends Neurosci.* **38**, 86–95 (2015).
- Ceko, M. *et al.* Partial recovery of abnormal insula and dorsolateral prefrontal connectivity to cognitive networks in chronic low back pain after treatment. *Hum Brain Mapp.* **36**, 2075–2092 (2015).
- Hemington, K. S., Wu, Q., Kucyi, A., Inman, R. D. & Davis, K. D. Abnormal cross-network functional connectivity in chronic pain and its association with clinical symptoms. *Brain Struct Funct.* (2015) (doi:10.1007/s00429-015-1161-1).
- Baliki, M. N., Mansour, A. R., Baria, A. T. & Apkarian, A. V. Functional reorganization of the default mode network across chronic pain conditions. *PLoS One* **9**, e106133 (2014).
- Kucyi, A., Salomons, T. V. & Davis, K. D. Mind wandering away from pain dynamically engages antinociceptive and default mode brain networks. *Proc Natl Acad Sci. USA* **110**, 18692–18697 (2013).
- Makin, T. R. *et al.* Network-level reorganisation of functional connectivity following arm amputation. *NeuroImage* **114**, 217–225 (2015).
- McKlveen, J. M., Myers, B. & Herman, J. P. The medial prefrontal cortex: coordinator of autonomic, neuroendocrine and behavioural responses to stress. *J Neuroendocrinol.* **27**, 446–456 (2015).
- Bushnell, M. C., Ceko, M. & Low, L. A. Cognitive and emotional control of pain and its disruption in chronic pain. *Nat Rev Neurosci.* **14**, 502–511 (2013).
- Seminowicz, D. A. & Davis, K. D. Pain enhances functional connectivity of a brain network evoked by performance of a cognitive task. *J Neurophysiol* **97**, 3651–3659 (2007).
- Seidel, E. M. *et al.* Uncertainty during pain anticipation: the adaptive value of preparatory processes. *Hum Brain Mapp.* **36**, 744–755 (2015).
- Seeley, W. W. *et al.* Dissociable intrinsic connectivity networks for salience processing and executive control. *J Neurosci.* **27**, 2349–2356 (2007).
- Spreng, R. N., Sepulcre, J., Turner, G. R., Stevens, W. D. & Schacter, D. L. Intrinsic architecture underlying the relations among the default, dorsal attention, and frontoparietal control networks of the human brain. *J Cogn Neurosci.* **25**, 74–86 (2013).
- Whitburn, L. Y., Jones, L. E., Davey, M. A. & Small, R. Women's experiences of labour pain and the role of the mind: an exploratory study. *Midwifery* **30**, 1029–1035 (2014).
- Gagua, T., Tkeshelashvili, B., Gagua, D. & McHedlishvili, N. Assessment of anxiety and depression in adolescents with primary dysmenorrhea: a case-control study. *J Pediatr Adolesc Gynecol.* **26**, 350–354 (2013).
- Zang, Y., Jiang, T., Lu, Y., He, Y. & Tian, L. Regional homogeneity approach to fMRI data analysis. *NeuroImage* **22**, 394–400 (2004).
- Zhong, Y. *et al.* Altered regional synchronization in epileptic patients with generalized tonic-clonic seizures. *Epilepsy Res.* **97**, 83–91 (2011).
- Iwabuchi, S. J. *et al.* Localized connectivity in depression: A meta-analysis of resting state functional imaging studies. *Neurosci Biobehav Rev.* **51**, 77–86 (2015).
- Yan, F. X. *et al.* Resting-state functional magnetic resonance imaging analysis with seed definition constrained by regional homogeneity. *Brain Connect.* **3**, 438–449 (2013).
- Roy, M., Shohamy, D. & Wager, T. D. Ventromedial prefrontal-subcortical systems and the generation of affective meaning. *Trends Cogn sci.* **16**, 147–156 (2012).
- Hsieh, J. C., Stone-Elender, S. & Ingvar, M. Anticipatory coping of pain expressed in the human anterior cingulate cortex: a positron emission tomography study. *Neurosci Lett.* **262**, 61–64 (1999).
- Woo, C. W., Roy, M., Buhle, J. T. & Wager, T. D. Distinct brain systems mediate the effects of nociceptive input and self-regulation on pain. *PLoS Biol.* **13**, e1002036 (2015).
- Kucyi, A. *et al.* Enhanced medial prefrontal-default mode network functional connectivity in chronic pain and its association with pain rumination. *J Neurosci.* **34**, 3969–3975 (2014).
- Napadow, V. *et al.* Intrinsic brain connectivity in fibromyalgia is associated with chronic pain intensity. *Arthritis Rheum.* **62**, 2545–2555 (2010).
- Loggia, M. L. *et al.* Default mode network connectivity encodes clinical pain: an arterial spin labeling study. *Pain* **154**, 24–33 (2013).
- Garcia-Larrea, L. & Peyron, R. Pain matrices and neuropathic pain matrices: a review. *Pain* **154**, Suppl 1, S29–43 (2013).
- Kutch, J. J. & Tu, F. F. Altered brain connectivity in dysmenorrhea: pain modulation and the motor cortex. *Pain* **157**, 5–6 (2016).
- Bosch, O. G. *et al.* Sleep deprivation increases dorsal nexus connectivity to the dorsolateral prefrontal cortex in humans. *Proc Natl Acad Sci. USA* **110**, 19597–19602 (2013).
- Hermans, E. J., Henckens, M. J., Joels, M. & Fernandez, G. Dynamic adaptation of large-scale brain networks in response to acute stressors. *Trends Neurosci.* **37**, 304–314 (2014).
- Hong, J. Y. *et al.* Sex and disease-related alterations of anterior insula functional connectivity in chronic abdominal pain. *J Neurosci.* **34**, 14252–14259 (2014).
- Pannekoek, J. N. *et al.* Resting-state functional connectivity abnormalities in limbic and salience networks in social anxiety disorder without comorbidity. *Eur Neuropsychopharmacol.* **23**, 186–195 (2013).
- Lorenz, J., Minoshima, S. & Casey, K. L. Keeping pain out of mind: the role of the dorsolateral prefrontal cortex in pain modulation. *Brain* **126**, 1079–1091 (2003).
- Spreng, R. N. *et al.* Goal-congruent default network activity facilitates cognitive control. *J Neurosci.* **34**, 14108–14114 (2014).
- Ochsner, K. N., Silvers, J. A. & Buhle, J. T. Functional imaging studies of emotion regulation: a synthetic review and evolving model of the cognitive control of emotion. *Ann N Y Acad sci.* **1251**, E1–24 (2012).

48. Downar, J., Mikulis, D. J. & Davis, K. D. Neural correlates of the prolonged salience of painful stimulation. *NeuroImage* **20**, 1540–1551 (2003).
49. Apkarian, A. V., Bushnell, M. C., Treede, R. D. & Zubieta, J. K. Human brain mechanisms of pain perception and regulation in health and disease. *Eur J Pain* **9**, 463–484 (2005).
50. Wiech, K., Jbabdi, S., Lin, C. S., Andersson, J. & Tracey, I. Differential structural and resting state connectivity between insular subdivisions and other pain-related brain regions. *Pain* **155**, 2047–2055 (2014).
51. Kutch, J. J. *et al.* Altered resting state neuromotor connectivity in men with chronic prostatitis/chronic pelvic pain syndrome: A MAPP: Research Network Neuroimaging Study. *NeuroImage Clin* **8**, 493–502 (2015).
52. Humphreys, G. F. & Lambon Ralph, M. A. Fusion and Fission of Cognitive Functions in the Human Parietal Cortex. *Cereb Cortex* **25**, 3547–3560 (2015).
53. Wiech, K., Ploner, M. & Tracey, I. Neurocognitive aspects of pain perception. *Trends Cogn sci.* **12**, 306–313 (2008).
54. Salomons, T. V., Moayed, M., Erpelding, N. & Davis, K. D. A brief cognitive-behavioural intervention for pain reduces secondary hyperalgesia. *Pain* **155**, 1446–1452 (2014).
55. Grant, J. A., Courtemanche, J. & Rainville, P. A non-elaborative mental stance and decoupling of executive and pain-related cortices predicts low pain sensitivity in Zen meditators. *Pain* **152**, 150–156 (2011).
56. Craig, A. D. Interoception: the sense of the physiological condition of the body. *Curr Opin Neurobiol.* **13**, 500–505 (2003).
57. Berntson, G. G. *et al.* The insula and evaluative processes. *Psychol sci.* **22**, 80–86 (2011).
58. Wiech, K. *et al.* Anterior insula integrates information about salience into perceptual decisions about pain. *J Neurosci.* **30**, 16324–16331 (2010).
59. Desbordes, G. *et al.* Evoked itch perception is associated with changes in functional brain connectivity. *NeuroImage Clin* **7**, 213–221 (2015).
60. Gorka, S. M., Fitzgerald, D. A., de Wit, H., Angstadt, M. & Phan, K. L. Opioid modulation of resting-state anterior cingulate cortex functional connectivity. *J Psychopharmacol.* **28**, 1115–1124 (2014).
61. Dennis, E. L., Gotlib, I. H., Thompson, P. M. & Thomason, M. E. Anxiety modulates insula recruitment in resting-state functional magnetic resonance imaging in youth and adults. *Brain Connect* **1**, 245–254 (2011).
62. Wiech, K. *et al.* Dissociable neural mechanisms underlying the modulation of pain and anxiety? An fMRI pilot study. *Plos One* **9**, e110654 (2014).
63. Fontana, D. & Rees, V. Primary dysmenorrhea, educational performance, and cognitive and affective variables in adolescent schoolgirls. *Br J Educ Psychol.* **52**, 199–204 (1982).
64. Pecina, M. *et al.* Valence-specific effects of BDNF Val66Met polymorphism on dopaminergic stress and reward processing in humans. *J Neurosci.* **34**, 5874–5881 (2014).
65. Lui, S. *et al.* High-field MRI reveals an acute impact on brain function in survivors of the magnitude 8.0 earthquake in China. *Proc Natl Acad Sci. USA* **106**, 15412–15417 (2009).
66. Petersen, N., Kilpatrick, L. A., Goharзад, A. & Cahill, L. Oral contraceptive pill use and menstrual cycle phase are associated with altered resting state functional connectivity. *NeuroImage* **90**, 24–32 (2014).
67. Chao-Gan, Y. & Yu-Feng, Z. DPARSF: A MATLAB Toolbox for “Pipeline” Data Analysis of Resting-State fMRI. *Front Syst Neurosci.* **4**, 13 (2010).
68. Hu, S. *et al.* Association of cerebral networks in resting state with sexual preference of homosexual men: a study of regional homogeneity and functional connectivity. *Plos One* **8**, e59426 (2013).
69. Weissenbacher, A. *et al.* Correlations and anticorrelations in resting-state functional connectivity MRI: a quantitative comparison of preprocessing strategies. *NeuroImage* **47**, 1408–1416 (2009).
70. Buckner, R. L., Krienen, F. M. & Yeo, B. T. Opportunities and limitations of intrinsic functional connectivity MRI. *Nat Neurosci.* **16**, 832–837 (2013).
71. Fox, M. D., Zhang, D., Snyder, A. Z. & Raichle, M. E. The global signal and observed anticorrelated resting state brain networks. *J Neurophysiol.* **101**, 3270–3283 (2009).
72. Murphy, K., Birn, R. M., Handwerker, D. A., Jones, T. B. & Bandettini, P. A. The impact of global signal regression on resting state correlations: are anti-correlated networks introduced? *NeuroImage* **44**, 893–905 (2009).
73. Ku, H. L. *et al.* Brain signature characterizing the body-brain-mind axis of transsexuals. *Plos One* **8**, e70808 (2013).
74. Fischl, B. & Dale, A. M. Measuring the thickness of the human cerebral cortex from magnetic resonance images. *Proc Natl Acad Sci. USA* **97**, 11050–11055 (2000).
75. Raichle, M. E. The restless brain. *Brain Connect* **1**, 3–12 (2011).

Acknowledgements

This study was supported by Taipei Veterans General Hospital (V100D-001, V100D-001-1, V100D-001-2), Ministry of Science and Technology (NSC 100-2314-B-010-006-MY3, NSC 100-2629-B-010-001, NSC 101-2629-B-010-001, NSC 102-2629-B-010-001, MOST 103-2321-B-010-020, MOST 104-2321-B-010-006), TVGH-NTUH joint research program (VN-103-05, VN-104-03), and The Aim for the Top University Plan of the Ministry of Education for National Yang-Ming University.

Author Contributions

C.H.T., L.F.C. and J.C.H. conceived and designed the experiments. W.C.L., I.L., C.H.T. and C.Y.C. performed the experiments. T.H.W. analyzed the data. C.H.T., T.C.Y., C.M.C., C.C.C. and L.F.C. contributed reagents/materials/analysis tools. H.T.C. performed clinical Assessment. T.H.W., C.H.T. and J.C.H. wrote the paper. All authors reviewed the manuscript. J.C.H. approved the final submission.

Additional Information

Supplementary information accompanies this paper at <http://www.nature.com/srep>

Competing financial interests: The authors declare no competing financial interests.

How to cite this article: Wu, T.-H. *et al.* Dynamic Changes of Functional Pain Connectome in Women with Primary Dysmenorrhea. *Sci. Rep.* **6**, 24543; doi: 10.1038/srep24543 (2016).



This work is licensed under a Creative Commons Attribution 4.0 International License. The images or other third party material in this article are included in the article’s Creative Commons license, unless indicated otherwise in the credit line; if the material is not included under the Creative Commons license, users will need to obtain permission from the license holder to reproduce the material. To view a copy of this license, visit <http://creativecommons.org/licenses/by/4.0/>